Biophysical Chemistry 185 (2014) 88–97

Contents lists available at ScienceDirect

Biophysical Chemistry

journal homepage: http://www.elsevier.com/locate/biophyschem

# Conformational dissection of *Thermomyces lanuginosus* lipase in solution

Karen M. Gonçalves [a,b], Leandro R.S. Barbosa [c], Luís Maurício T.R. Lima [a,d], Juliana R. Cortines [e], Dário E. Kalume [f], Ivana C.R. Leal [a], Leandro S. Mariz e Miranda [b], Rodrigo O.M. de Souza [b], Yraima Cordeiro [a,*]

[a] Faculdade de Farmácia, Universidade Federal do Rio de Janeiro, Rio de Janeiro, RJ 21941-902, Brazil
[b] Instituto de Química, Universidade Federal do Rio de Janeiro, Centro de Tecnologia, Rio de Janeiro, RJ, Brazil
[c] Instituto de Física, Universidade de São Paulo, SP, Brazil
[d] Laboratory for Structural Biology (DIMAV), Brazilian National Institute of Metrology, Quality and Technology—INMETRO, Duque de Caxias, RJ 25250-020, Brazil
[e] Departamento de Virologia, Instituto de Microbiologia Paulo de Góes, Universidade Federal do Rio de Janeiro, Rio de Janeiro, RJ 21941-590, Brazil
[f] Laboratório Interdisciplinar de Pesquisas Médicas, Instituto Oswaldo Cruz, Fundação Oswaldo Cruz, Rio de Janeiro, RJ 21040-360, Brazil

## HIGHLIGHTS

- The conformation and oligomeric state of a commercial lipase (TLL) were evaluated.
- SAXS data evidenced the presence of monomers and dimers of TLL in solution.
- Mass spectrometry analysis confirmed that TLL is present in both forms.
- The presence of dimeric species might compromise overall enzyme activity.

## GRAPHICAL ABSTRACT

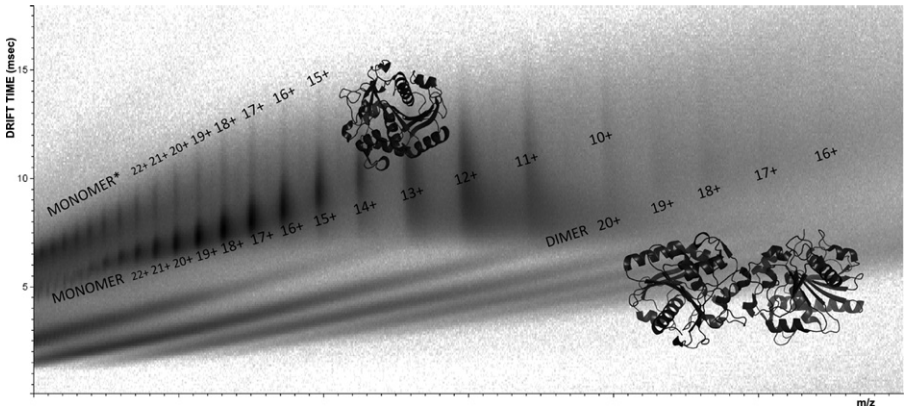


## ARTICLE INFO

*Article history:*
Received 30 October 2013
Received in revised form 2 December 2013
Accepted 4 December 2013
Available online 14 December 2013

*Keywords:*
Lipase
Oligomer
Small angle x-ray scattering
Ion mobility mass spectrometry
Circular dichroism
Fluorescence

## ABSTRACT

Lipases are triacyl glycerol acyl hydrolases, which catalyze hydrolysis of esters, esterification and transesterification reactions, among others. Some of these enzymes have a large hydrophobic pocket covered by an alpha-helical mobile surface loop (the lid). Protein–protein interactions can occur through adsorption of two open lids of individual lipases. We investigated the conformation and oligomeric state of *Thermomyces lanuginosus* lipase (TLL) in solution by spectroscopic and mass spectrometry techniques. Information about oligomerization of this important industrial enzyme is only available for TLL crystals; therefore, we have done a throughout investigation of the conformation of this lipase in solution. SDS-PAGE and mass spectrometry analysis of size-exclusion chromatography eluted fractions indicated the presence of both monomeric and dimeric populations of TLL. The stability of the enzyme upon thermal and guanidine hydrochloride treatment was examined by circular dichroism and fluorescence emission spectroscopy. Small angle x-ray scattering and ion mobility mass spectrometry analysis revealed that TLL is found as a mixture of monomers and dimers at the assayed concentrations. Although previous x-ray diffraction data showed TLL as a dimer in the crystal (PDB: 1DT3), to our knowledge our report is the first evidencing that TLL co-exists as stable dimeric and monomeric forms in solution.



* Corresponding author at: Universidade Federal do Rio de Janeiro, Av. Carlos Chagas Filho 373, Faculdade de Farmácia, CCS, Bloco B, subsolo, sala 17, 21941-902, Rio de Janeiro, RJ, Brazil. Tel.: +55 21 2260 9192x210.
*E-mail address:* yraima@pharma.ufrj.br (Y. Cordeiro).

0301-4622/$ – see front matter © 2013 Elsevier B.V. All rights reserved.
http://dx.doi.org/10.1016/j.bpc.2013.12.001

## 1. Introduction

Lipases are carboxyl-esterases that catalyze the hydrolysis of long-chain acylglycerols [1]. Despite these enzymes are diverse in their amino acid sequences, previous crystallographic analysis revealed their typical α/β hydrolase scaffold, with catalytic residues constituted by a highly conserved trypsin-like triad of Ser–His–Asp(Glu) residues [2].

The lipase from *Thermomyces lanuginosus* (TLL) (previously *Humicola lanuginosa*) is obtained as a commercial soluble lipase preparation supplied by Novozymes® and is produced by a genetically modified strain of *Aspergillus oryzae*. The molar mass of this lipase is ~30 kDa, and it is mono-glycosylated at Asn33, which adds approximately 2 kDa to the final mass of the native enzyme [3]. The TLL has 269 amino acid residues in its primary sequence, four of which are tryptophan (89, 117, 221 and 260). Thus, an efficient method to follow the protein unfolding is to monitor Trp fluorescence upon application of physical or chemical variables [4]. Besides, as a consequence of the proximity of Trp89 to the active site, changes in its fluorescence emission can be related to conformational changes in the active site, specifically in the lid. Moreover, Trp89 seems to be important for the catalysis, while Trp residues 117, 221 and 260 have been reported to participate in the structural stability of *T. lanuginosus* lipase, as seen by steady-state and time resolved fluorescence spectroscopy of wild-type and TLL mutants [5].

X-ray diffraction studies showed that the TLL presents a central eight-stranded predominantly parallel β-sheet structure, with five interconnecting α-helices [2]. The lid is an α-helical mobile surface loop that covers the active site [2], and the catalytic triad of Ser146-Asp201-His258 is similar to those seen in serine proteases [5].

Despite that TLL crystallographic studies evidenced three distinct conformational states, an unstable intermediate form and two stable forms (closed and open lid conformations) [2], it is suggested that the enzyme conformation is closed in aqueous environments; thus, the access to the catalytic triad would be blocked by the lid. It was also shown that when TLL is bound to substrate analogs, the helix forming the lid is displaced and the active site becomes exposed [4].

In contrast, it was reported that lipases might crystallize in their open conformation without the presence of substrates or inhibitors, suggesting that exposition of hydrophobic areas surrounding the active center occurs in the unbound enzyme. The exposed large hydrophobic pocket can promote the association between two open lipases, hence enabling oligomer formation [6].

Dimerization of the lipase of *Pseudomonas fluorescens* was proposed previously [7]. Reduced activity was observed at higher enzyme concentrations, indicating that dimers are less active than monomers. Besides, when detergents such as Triton X were added in the solution, there was no difference in activities of preparations with different lipase concentration, indicating dissociation of dimers into monomers. The same behavior was observed for the lipase from *Alcaligenes* sp. [6]. Additionally, it was shown that *Alcaligenes* sp. lipase dimers were more stable to thermal denaturation than the monomers [6].

Some authors suggest that the *T. lanuginosus* and *Mucor miehei* (MML, Novozym® 388) lipases have a strong tendency to dimerize, even at very low protein concentrations [8,9]. However, the existence of TLL dimers in solution is still controversial, and the structure and conformation of this species were not evaluated in aqueous solution. Dimeric forms of these lipases were only investigated for immobilized enzymes, in the presence or absence of detergents, or by gel exclusion chromatography, mainly with enzyme concentrations higher than 300 μg/mL. Only a small percentage of dimers was found at lower concentrations (below 50 μg/mL) [8].

For the TLL, another indication of its tendency to form dimers (i.e., less active species) is the fact that solubilizing the enzyme in the presence of detergents leads to an increase in the activity by more than one order of magnitude [10]. This fact is not related to the interfacial activation, but rather to the dissociation of intermolecular interactions that keep the enzyme in the dimeric conformation.

Here we investigated the conformation and oligomeric state of the native *T. lanuginosus* lipase through size-exclusion chromatography (SEC), small angle x-ray scattering (SAXS) and Electrospray Ionization–Ion Mobility Spectrometry–Mass Spectrometry (ESI–IMS–MS) in aqueous phase. SAXS and ESI–IMS–MS techniques were employed to evaluate the conformation and oligomerization state of TLL in solution, since they are powerful tools to study biological systems in conditions close to physiological [11–14]. Moreover, the stability of the enzyme upon thermal and guanidine hydrochloride (GdnHCl) denaturation was investigated by circular dichroism (CD) and intrinsic fluorescence spectroscopy, to provide structure–stability relationships. Using such methodologies, the present study shows that TLL is present as a mixture of dimeric and monomeric states in solution.

## 2. Materials and methods

### 2.1. Materials

*T. lanuginosus* lipase (TLL) was obtained as crude extract from Novozymes® (Bagsvaerd, Denmark) and its concentration was determined by the Bradford method [15] or, for the purified enzyme, by its extinction coefficient at 280 nm (36,900 $M^{-1}$ $cm^{-1}$), calculated from the TLL primary sequence in http://web.expasy.org/protparam/. GdnHCl (99.9% pure) and the purified enzymes for SEC analysis were acquired from Sigma-Aldrich (St. Louis, MO, USA). Buffers used in the experiments were sodium phosphate and tris(hydroxymethyl) aminomethane from VETEC (Duque de Caxias, RJ, Brazil). The SDS-PAGE standard used was Precision Plus Protein™ Dual Color (Bio-Rad, CA, USA), containing a mixture of 10 recombinant proteins (from 10 to 250 kDa).

### 2.2. Size-exclusion chromatography (SEC)

The enzyme was purified by SEC using TSK gel 3000 (7.5 mm ID × 30 cm × 10 μm) (TosoH Corp., Tokyo, Japan) or Superdex 75 10/300 GL (GE Healthcare, USA) columns in a Jasco PU 2089 Plus chromatograph (Jasco Corp., Japan). Elution was done in 50 mM phosphate buffer, pH 7.0, at flow rates of 1.0 mL/min or 0.5 mL/min for TSK or Superdex columns, respectively. The collected aliquots were analyzed by SDS-PAGE (12.5%) and further lyophilized. The calibration curve was made using the purified proteins from Sigma-Aldrich: lysozyme (14.3 kDa), carbonic anhydrase (29 kDa), ovalbumin (45 kDa), BSA (66 kDa) and β-amylase (200 kDa). The chromatographic run was monitored with a UV-absorption detector at 280 nm.

### 2.3. Enzyme activity

The lipase activity was determined as described by Invernizzi et al. [16]. The measurements were made by following the increase in absorbance at 410 nm generated by the release of *p*-nitrophenol produced by the hydrolysis of 5 mM *p*-nitrophenyl palmitate (dissolved in isopropanol) in 100 mM Tris–HCl buffer, pH 7.5, supplemented with 0.005% Triton X-100 at room temperature. The enzyme and substrate solution were heated separately at different temperatures and the reaction was started with the lipase addiction, as described [16].

### 2.4. Intrinsic and extrinsic fluorescence measurements

Fluorescence measurements were carried out in a Jasco FP 6300 spectrofluorimeter (Jasco Corp., Japan) with excitation set at 280 nm and emission was monitored from 300 to 420 nm. The center of spectral mass values ‹λ› of TLL fluorescence emission spectra were calculated

using the equation below (Eq. (1)), where $F_i$ is the fluorescence emitted at wavelength $\lambda_i$, and the summation is conducted over the range of appreciable values of $F$:

$$\langle\lambda\rangle = \sum \lambda_i F_i / \sum F_i \quad (1)$$

1,8 ANS fluorescence. A stock solution of 1-anilinonaphthalene-8-sulfonic acid (1,8-ANS) (Sigma-Aldrich, USA) was prepared at 500 μM in methanol. TLL samples at 4 μM in 100 mM Tris–HCl buffer, pH 7.5, containing 1,8 ANS at 40 μM were incubated in the presence of increasing GdnHCl concentrations for 10 min prior to measurements. 1,8 ANS binding to TLL was investigated by exciting samples at 360 nm and recording emission from 400 to 600 nm.

### 2.5. Circular dichroism (CD)

Far-UV CD spectra (250–190 nm) were recorded in a Chirascan spectropolarimeter (Applied Photophysics, UK) coupled to a thermal bath, with temperature controlled with a Peltier device. TLL samples were analyzed at 100 μg/mL in 100 mM sodium phosphate buffer, pH 7.0 in a 2.00 mm path-length quartz cuvette. For thermal-induced unfolding, the ellipticity value at 222 nm was recorded while the temperature was increased at 1 °C/min (from 25 to 90 °C). A CD spectrum (250–190 nm) was collected at every 5 °C.

### 2.6. Thermal and guanidine hydrochloride denaturation

The stability of the enzyme upon physical (temperature increase) and chemical (GdnHCl addition) treatments was investigated by CD and fluorescence emission spectroscopy. Native protein samples were prepared in 100 mM phosphate buffer (pH 7.0) at 1.0 mg/mL and rapidly diluted (10 fold) into solutions with increasing GdnHCl concentrations. The final enzyme concentration was 100 μg/mL in all samples. Conformational changes upon unfolding were monitored by tryptophan fluorescence emission (excitation at 280 nm) and by Far-UV CD (from 250 to 190 nm), as described in previous items of the Methods section.

### 2.7. Small angle x-ray scattering (SAXS)

Small angle x-ray scattering (SAXS) experiments were performed at the SAXS2 beamline of the Brazilian Synchrotron Light Laboratory (LNLS, SP, Brazil). A monochromatic X-ray beam was used ($\lambda = 1.488$ Å) with the sample to detector distance set at ~975 mm. Scattering data were recorded (each frame collected for 300 s) using a two-dimensional position-sensitive MARCCD detector. The SAXS curves were corrected by the buffer scattering taking into account the sample's attenuation. The raw extract of *T. lanuginosus* enzyme was analyzed at 27 mg/mL, and the TLL diluted in 100 mM Tris–HCl buffer, pH 7.0, was analyzed at 5.4 and 2.7 mg/mL final concentrations.

Briefly, the SAXS intensity, $I(q)$, of an isotropic solution of non-interacting scattering particles can be described as [17–19]:

$$I(q) = k\ n_p P(q) \quad (2)$$

where $n_p$ corresponds to the particle number density and $k$ is an unknown factor related to instrumental effects ($q = 4\pi sin\theta/\lambda$ is the scattering vector, being $2\theta$ as the scattering angle). $P(q)$ in Eq. (2), gives information about the scattering particle size and shape and it is known as the particle form factor. Noteworthy, considering the methodology applied in the present study, $k$ must be the same for different scattering curves acquired with the same experimental setup.

The pair distance distribution function, $p(r)$, can be extracted from the experimental scattering curve using the Indirect Fourier Transform (IFT) methodology, which can be applied in the case of non-interacting systems [17–19] (Eq. (2)). The $p(r)$ function provides the structural features of the scattering particles, such as the particle maximum dimension, $D_{max}$, and its radius of gyration, $R_g$. In the current study, we used GNOM software [20,21] to generate the $p(r)$ functions from the experimental $I(q)$ curves.

Besides, in order to calculate the theoretical protein form factors, $P(q)$, and to fit the experimental data, GENFIT software [22–24] was employed. This methodology assumes that the protein crystallographic structure is known and follows the procedure described in Ortore et al. [25]. This is a very efficient and precise methodology to calculate the protein scattering curve [22–26]. However, one should bear in mind that it assumes that the protein tertiary structure in the crystal (PDB file) and in solution are the same. Details are described elsewhere [23,25].

As it will be shown later in the text, there are some cases when the protein scattering curve will be described as a sum of monomers and dimers (PDB: 1DT3) in solution. In such data analysis the effective form factor of scattering particles is given by a weighted sum of the form factor of the dimers, $P_D(q)$ and monomers, $P_M(q)$ (Eq. (3)); both form factors were calculated and fitted to the experimental SAXS curve using GENFIT software [23–26].

Following this methodology and assuming that the interactions between monomer–monomer, dimer–dimer and monomer–dimer can be neglected, the scattering intensity of a sample composed of monomers and dimers in equilibrium, i.e., the total amount of each population does not change along time, can be written as (Eq. (3)):

$$I(q) = kn_p\left\{W_D P_M(q) + \frac{(1-W_M)}{2} P_D(q)\right\} \quad (3)$$

where $n_p$ is the protein concentration, $w_M$ is the amount of protein in the monomeric form, and $P_M(q)$, $P_D(q)$ are the monomer and dimer theoretical form factors, respectively. This SAXS analysis was performed with GENFIT software, as described [25]. Besides, the Global Fit procedure (GENFIT software) allows the analysis of several scattering curves concomitantly [22–26], connecting different parameters of different scattering curves. Following such methodology, both $k$, which must be the same for the scattering curves, as well as $w_M$ are only fitting parameters. Besides, the experimental factor $k$ was kept the same for the SAXS curves of TLL at 2.7 and 5.4 mg/mL, during the $\chi^2$ minimization. Further details can be found in [26].

The best solution was then obtained by minimizing the reduced $\chi^2$ [23–26], in a simulated annealing process [27]. By doing so, a value of $k = (2.51 \pm 0.03)\ x\ 10^{-2}$ was obtained for the two SAXS curves, which corresponds to the common unknown instrumental factor (Eq. (2)). Thus, this methodology was able to calculate the unknown experimental factor $k$, within a ~1% variation.

### 2.8. In-gel digestion (IGD) and mass spectrometry analysis of excised bands

TLL samples (after SEC and the raw extract) were analyzed in a 12.5% SDS-PAGE and stained with coomassie brilliant blue. The bands corresponding to the monomer (~30 kDa) and dimer (~50 kDa) were excised. In-gel digestion was performed as described in the University of San Francisco IGD protocol (http://msf.ucsf.edu/ingel.html). Briefly, 30 μL of Trypsin Gold, Mass Spectrometry Grade (Promega, WI, USA) was added to cover the dried gel pieces and the reaction was allowed to proceed at 37 °C for 16 h. The aqueous-extracted peptides were collected and placed in fresh tubes. To the gel pieces, 50% acetonitrile/5% formic acid was added, incubated for 30 min in a vortex and sonicated for 5 min to enhance peptide recovery. The digested sample was loaded onto a 100 μm × 100 μm C18 column and analyzed in a Micromass Q-ToF micro (Waters Corporation, USA) at the UEMP, UFRJ. This procedure was performed for both the monomer and dimer bands.

MS/MS data obtained were analyzed using the web-based Mascot tool MS/MS Ion Search (www.matrixscience.com), using the SwissProt database, under all taxonomic categories. As for the peptide search, two missed trypsin cleavages were allowed, mass tolerance was

1.2 Da for precursor ions and 0.6 Da for daughter ions, and no modifications were included on the search. The significance threshold for protein family determination was $P < 0.05$.

### 2.9. Matrix-assisted laser desorption and ionization-time-of-flight mass spectrometry (MALDI-ToF-MS)

The main peak eluted from SEC was analyzed by MALDI-ToF-MS by mixing equal volumes of 0.07 mM TL lipase with 50% acetonitrile in water containing 0.1% trifluoroacetic acid (TFA) and 10 mg/mL sinapinic acid. Samples were then spotted onto a stainless steel plate and subjected to MALDI-ToF-MS in an Aulex Speed spectrometer (Bruker, USA) in positive linear mode. Data were exported and analyzed using mMass [28].

### 2.10. Electrospray ionization–ion mobility spectrometry–mass spectrometry (ESI–IMS–MS)

Measurements were performed in a SYNAPT High Definition Mass Spectrometer (HDMS) (Waters, Brazil). TLL samples were diluted to 158 μg/mL (5 μM) in 100 mM ammonium acetate buffer pH 7.0 and injected at a rate of 10 μL/min. Measurements were performed in positive ESI mode, with a capillary voltage of 3.0 kV and N2 at 0.4 bar. Data processing was performed for 8 min accumulation, from data acquired over the range of m/z 1,000 to 4,000 with repeated 3 s acquisition time per point. Mass calibration was routinely performed with GFP cleavage peptides mass spectrometry standard (Waters). Other typical instrumental settings are as described previously [14]. Data were analyzed using DriftScope 2.1 (Waters Corporation, Brazil) [29]. The deconvolution of the mass spectra was conducted by using the MaxEnt 1 algorithm as implemented in the MassLynx software.

## 3. Results and discussion

### 3.1. Analysis of purified T. lanuginosus lipase (TLL) by SDS-PAGE and mass spectrometry

For carrying out the thermal and chemical stability studies, TLL was purified from the commercial solution by SEC in TSK 3000 or Superdex 75 columns. Absorbance was followed at 280 nm and a major intense elution peak was observed (Fig. 1A, peak 2), preceded by a small peak (Fig. 1). The estimated hydrodynamic radii ($R_h$) of the species eluted in the main peak and in the first peak (lower retention time) were 28.8 Å and 30.2 Å, respectively (Fig. 1A); this estimative was obtained from a calibration curve generated with standard proteins, as described elsewhere [30]. The integral area of SEC was calculated using the Fityk software [31]. The monomer/dimer ratio was 20.7, which means that at a final calculated concentration of 111 μg/mL, TLL is populated as 95.4% monomers and 4.6% dimers.

SDS-PAGE (12.5%) analysis of the SEC-collected samples and the native TLL showed two major bands, one around 50 kDa and the other between 25 and 37 kDa (Fig. 1B); according to TLL's primary sequence, the expected molecular masses for monomer and dimer are 29.3 kDa and 58.6 kDa, respectively. Band intensity analysis of the native TLL in SDS-PAGE (Fig. 1B, lane 6) using ImageJ software [32], revealed a monomer/dimer ratio of 3.34, meaning that, at 200 μg/mL, TLL is present in the monomeric form at 77% and at 23% in the dimeric form.

To verify if the higher molecular weight species observed in the SDS-PAGE (and eluted after SEC) belongs to a TLL dimer, in-gel digestion of excised bands was performed as described in the Materials and Methods section. Samples were further analyzed by electrospray ionization quadrupole time-of-flight mass spectrometry (ESI-Q-TOF). We obtained 56% and 46% sequence coverage for the monomer and ~50 kDa (possible TLL dimer) excised bands, respectively. A MASCOT database search (www.matrixscience.com) defined the peptides as corresponding to the lipase from *T. lanuginosus*, supporting our hypothesis that

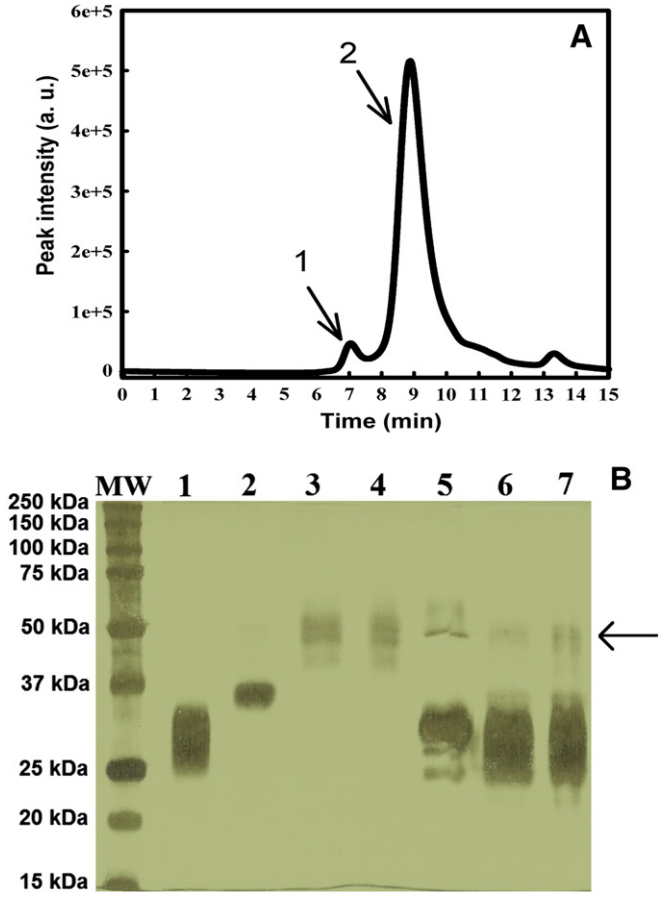


**Fig. 1.** Size exclusion chromatography and SDS-PAGE analysis of purified TLL samples. A. SEC profile of *Thermomyces lanuginosus* lipase in a TSK gel column (absorbance: 280 nm). Elution was done with a flow rate of 1.0 mL/min in 50 mM phosphate buffer, pH 7.0. Numbers 1 and 2 refer to collected samples that were applied in the SDS-PAGE. B. Molecular weight analysis of eluted fractions collected after SEC by SDS-PAGE. SEC-eluted samples were resolved in 12.5% SDS-PAGE and silver-stained. The first lane corresponds to the molecular weight markers (MW values are shown in the left, offset). 1, fraction eluted at 10–12 min; 2, fraction eluted at 8–10 min; 3 and 4, fractions eluted at 6–8 min; 5, denatured and boiled TLL at 200 μg/mL; 6 and 7, native TLL at 200 μg/mL. Fractions collected from SEC were not treated with β-mercaptoethanol. The arrow (lanes 3 to 7) indicates the TLL SDS-resistant dimer.

the band observed at ~50 kDa corresponds to TLL dimers. Moreover, our data indicate that the TLL dimer is SDS-resistant, as this band was observed in denaturing conditions in the SDS-PAGE. This behavior is not uncommon, it was already reported that even the monomeric form of TLL is SDS-resistant [33], and detergent-resistant dimers were also observed for other proteins, such as β-glycosidase [34].

To confirm that the purified fraction contained native lipase, activity measurements were done revealing 0.2 U/mg of hydrolytic activity for the monomer, using *p*-nitrophenyl palmitate as a substrate. This value was consistent with other studies, considering the lower enzyme concentration used in our study [35,36].

### 3.2. Thermal stability: structure–activity relationship

TLL thermal stability (heating up to 90 °C) was evaluated by far-UV circular dichroism and activity measurements. Far-UV CD spectra presented dominance of characteristic signals of α-helices and the secondary structure changes were monitored at 222 nm. There was a loss of only ~10% of the native secondary structure at 65 °C, while at 87 °C the enzyme lost 50% of its secondary structure content (Fig. 2A). Deconvolution of the CD spectra using different algorithms [37–39] showed that the α-helical content was reduced when temperature

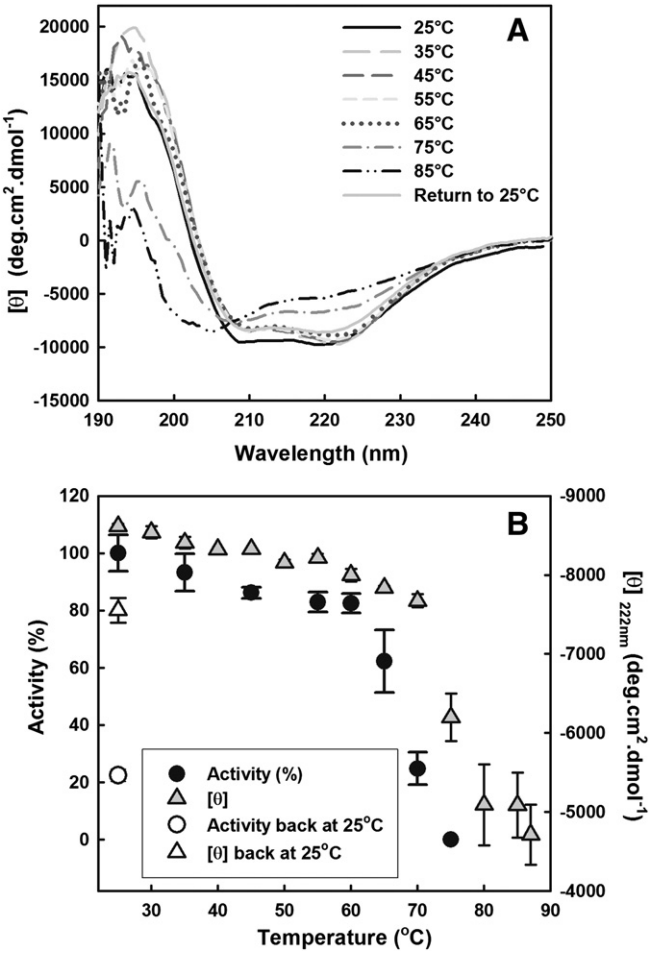


**Fig. 2.** Structure and activity changes of TLL upon thermal unfolding. A. Thermal stability of TLL evaluated by circular dichroism. The temperature was increased at 1 °C/min (from 25 to 90 °C) and a CD spectrum was collected at every 5 °C. After achieving the highest temperature, the enzyme solution (at 100 μg/mL in 50 mM phosphate buffer, pH 7.0) was cooled back to 25 °C. B. Enzyme activity data were obtained by *p*-nitrophenyl palmitate hydrolysis and the activity at 25 °C was determined as 100%. One international unit of activity (U) is defined as the mass (grams) of enzyme that hydrolyzes 1 μmol of *p*-nitrophenyl palmitate per minute under the conditions described in the Methods section. CD molar ellipticity values at 222 nm [θ] were monitored to follow protein unfolding.

was increased to 85 °C, while the β-sheet content increased (Table S1). The gain in β-sheets indicates that TLL is suffering temperature-induced aggregation (build up of intermolecular interactions), as previously observed for other proteins [40]. It is important to stress that, although deconvolution can provide information about secondary structure elements, we have focused our analysis in the overall protein conformational changes. Although a gradual loss in α-helical secondary structure was observed when temperature was increased to 90 °C, the high thermal stability of TLL was evidenced by a $T_m$ of 73.6 ± 0.8 °C (calculated from the plot shown in Fig. 2B). These results are consistent with previous CD and differential scanning calorimetry studies [41].

These secondary structure changes were correlated with the hydrolytic activity of the lipase at studied temperatures (Table 1). Activity measurements showed that *p*-nitrophenyl palmitate hydrolysis did not change significantly up to ~60 °C (Fig. 2B). Small conformational changes would compromise the functionality of this lipase, as observed at 65 °C, where while activity decreased to 62%, only ~10% of the native secondary structure was lost (Fig. 2A). Although the enzyme still retained part of its native secondary structure at high temperatures (Table S1), no activity was detected at 75 °C (Table 1). Even though the CD spectrum of TLL after return to 25 °C showed major recovery of its native secondary structure (Fig. 2A), as also described previously

**Table 1**
Thermal-dependent activity of TL lipase.

| Temperature (°C) | Activity (%) |
|---|---|
| 25 °C | 100 ± 6.3[b] |
| 35 °C | 93.2 ± 6.5 |
| 45 °C | 86.2 ± 2.0 |
| 55 °C | 82.9 ± 3.4 |
| 60 °C | 82.4 ± 3.4 |
| 65 °C | 62.3 ± 10.9 |
| 70 °C | 24.8 ± 5.7 |
| 75 °C | n.d.[c] |
| 25°C[a] | 22.4 ± 2.1 |

Activity was measured as the hydrolysis of 5 mM *p*-nitrophenyl palmitate, as described in the Material and Methods section.
[a] After cooling back to 25 °C.
[b] Activity considered 100% was 0.164 ± 0.01 U/mg. The final TLL concentration was 41 μg/mL.
[c] Non-detected.

[41], only 22% of the initial TLL activity was observed (Table 1, Fig. 2B). This result might be explained by subtle conformational changes that are important for the enzyme activity. Structural changes caused by high temperatures might take place close to the TLL active site, explaining the substantial loss in activity after the temperature curve.

### 3.3. Unfolding of TLL by guanidine hydrochloride

The unfolding of TLL was observed by incubation with the denaturant agent guanidine hydrochloride (GdnHCl). Changes in the secondary structure of the enzyme were observed by CD upon incubation with GdnHCl at increasing concentrations (Fig. 3A). A slight increase in the secondary structure content (4 to 6%) was observed at low GdnHCl concentrations (up to 2 M), suggesting population of an intermediate state, which could be in a molten globule conformation [42,43]. Above 3 M GdnHCl, a cooperative unfolding process was observed, suggesting that complete unfolding was achieved at ~5 M of chemical denaturant.

Evaluation of the changes in the fluorescence emission of TLL tryptophan residues is useful to follow protein folding and stability. The Trp residue located at position 89, in the lid, is responsible for 60% of TLL emission fluorescence [44], and this behavior is a consequence of the low fluorescence emission of the other three Trp residues (Trp117, Trp221, and Trp260), as described [45]. We have thus evaluated TLL tertiary structure changes induced by chemical unfolding with GdnHCl (Fig. 3B). A red-shift of the TLL fluorescence emission spectrum upon incubation with increasing GdnHCl concentrations was observed (Fig. 3B). This shift reveals an increased average exposure of tryptophan residues to the aqueous phase.

Changes in center of spectral mass values, i.e., changes in the Trp environment, were correlated with loss of ellipticity at 222 nm (Fig. 3C), showing that the enzyme loses both secondary and tertiary structure cooperatively and concomitantly upon GdnHCl unfolding. The values of [GdnHCl] corresponding to the midpoints of the transition curves ($G_{1/2}$) were 3.78 ± 0.03 M and 3.86 ± 0.04 M, from fluorescence and CD data, respectively (Fig. 3C). Our fluorescence data are consistent with previous intrinsic fluorescence and anisotropy measurements, which showed that the effects of GdnHCl in the protein seem to be complete around 5 M of the chaotrope and the midpoint of transition was obtained with ~4 M GdnHCl [3,4].

Although TLL GdnHCl-induced unfolding proceeded as a two-state mechanism (native and unfolded) with no evidence for stable intermediate states (Fig. 3C), intermediate states were reported in previous work [4], but could only be detected with time-resolved techniques, as stopped-flow fluorescence spectroscopy.

To identify possible intermediate states during TLL unfolding that were not visualized by GdnHCl treatment, the enzyme was incubated with the fluorescent probe 1,8-ANS. This hydrophobic dye binds partially folded protein species and binding is accompanied by an increase in 1,8-ANS fluorescence emission [46]. Thus, based on the affinity of this

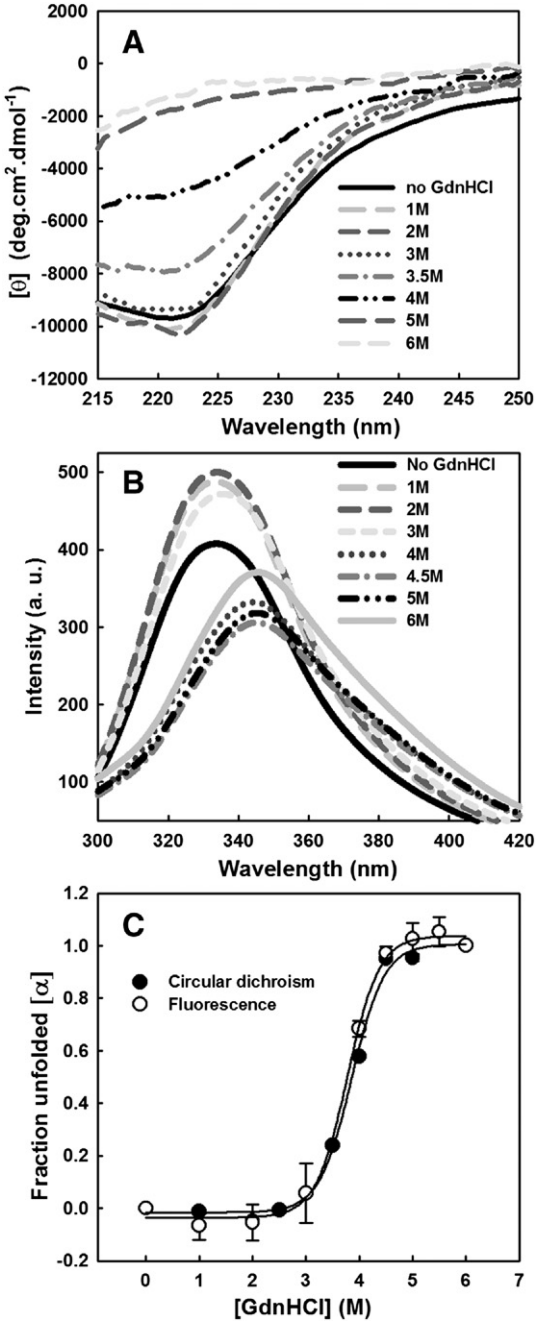


**Fig. 3.** Secondary and tertiary structure changes of TLL induced by chemical unfolding. A. Chemical unfolding of *Thermomyces lanuginosus* lipase followed by CD. TLL was incubated with increasing GdnHCl concentrations and, after 30 min incubation, CD spectra were recorded from 250 to 200 nm (data is only shown from 215 nm, as GdnHCl strongly absorbs below this wavelength). B. Chemical-induced TLL tertiary structure changes. Fluorescence emission spectra of TLL in the presence of increasing GdnHCl concentrations were recorded. Excitation was set at 280 nm. C. Effect of [GdnHCl] on the tertiary (fluorescence intensity) and secondary (CD) structure of TLL. Calculated $\Delta G^0$ was 9.05 and 8.35 kcal/mol from the fluorescence data and the CD data (assuming a two-state transition), respectively. Ellipticity values at 222 nm ($\varepsilon_{222nm}$) were collected and results are displayed as fraction unfolded ($\alpha$) ($\alpha = (\varepsilon_{222nmobs} - \varepsilon_{222nmI}) / (\varepsilon_{222nmF} - \varepsilon_{222nmI})$), where I stands for the initial value of $\varepsilon_{222nm}$ (in the absence of GdnHCl) and F stands for the final value of $\varepsilon_{222nm}$ (in 6 M GdnHCl). For the fluorescence emission we used the center of spectral mass values for calculation. TLL was analyzed at 100 μg/mL in 50 mM phosphate buffer, pH 7.0.

probe to highly non-polar environments, it is possible to follow conformational changes in proteins upon physical or chemical unfolding, and to characterize possible folding intermediates [47]. We observed a continuous increase in 1,8-ANS fluorescence emission at increasing GdnHCl concentrations (Fig. 4, inset), indicating that TLL did not unfold

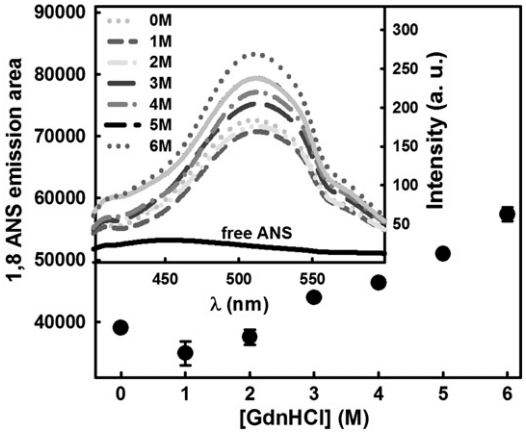


**Fig. 4.** 1,8-ANS fluorescence emission upon incubation with increasing GdnHCl concentrations. The TLL at 4 μM in 100 mM Tris–HCl buffer, pH 7.5, was incubated with 1,8 ANS at 40 μM under increasing concentrations of GdnHCl. The inset shows the emission spectra of 1,8-ANS in the presence of TLL at different GdnHCl concentrations or free in Tris–HCl buffer (solid black line). Emission spectra and the respective areas were corrected for 1,8-ANS fluorescence emission in the presence of the specified GdnHCl concentrations. Excitation was done at 360 nm and emission recorded from 400 to 600 nm.

completely even at high denaturing agent concentrations. Despite the fact that TLL loses secondary structure upon incubation with GdnHCl (Fig. 3A), there is still maintenance of residual structure even at 6 M GdnHCl. Besides, the increase in 1,8 ANS fluorescence could also be related to the presence of TLL dimers in solution. These oligomeric species would suffer GdnHCl-induced dissociation, and exposure of monomer–monomer interfaces would lead to increased binding of 1,8 ANS to TLL. The gradual increase in 1,8-ANS fluorescence with increasing GdnHCl concentrations (Fig. 4) excludes the possible presence of stable intermediate states for TLL; as shown for a cutinase from *Fusarium solani pisi* [48]. This result suggests that oligomeric species of TLL (such as dimers) are present in solution. Therefore, an increase in the fluorescence of the extrinsic probe could be related to dissociation of a dimer followed by partial unfolding of the monomers, with increased exposure of hydrophobic pockets.

### *3.4. Small angle x-ray scattering analysis of TLL in aqueous solution: evidence of co-existence of dimers and monomers*

Small angle X-ray scattering technique is a powerful tool to address the oligomeric and the conformational state of proteins in solution. The concentration-normalized scattering curves of TLL at 2.7 (circles) and 5.4 mg/mL (squares) are quite similar (Fig. 5A), evidencing that interference effects do not take place in the SAXS curves [23] at least in this concentration range. Analysis of the scattering curve of TLL raw extract (27 mg/mL), however, indicated a different behavior, where partial protein aggregation was probably taking place over the SAXS curves (Fig. S1). Such phenomenon was evidenced by an increase in the $R_g$ value in comparison with the diluted samples (Fig. S2). The SAXS data analysis of TLL is focused in the 2.7 and 5.4 mg/mL systems, where well-defined scattering curves were obtained.

The Kratky plot ($I(q)q^2 \times q$) is a useful tool in the SAXS data analysis of proteins in solution, since it can provide information about the whole macromolecular conformation [17,49]. Analysis of Kratky plots of TLL at 2.7 and 5.4 mg/mL (Fig. 5B) indicates that the enzyme is compact, presenting a globular shape, as evidenced by the bell-like shape of the peak at $q \sim 0.08$ Å$^{-1}$ [17,26,49].

The Guinier analysis [19] of TLL scattering curves at different concentrations (ranging from 27 to 2.7 mg/mL) yielded the calculation of $R_g$ (radius of gyration) values of 30.12 ± 0.14 Å for the commercial enzyme in the raw extract (Fig. S1). $R_g$ values of 26.50 ± 0.20 and 24.03 ± 0.14 Å were obtained for the TLL samples at 5.4 and

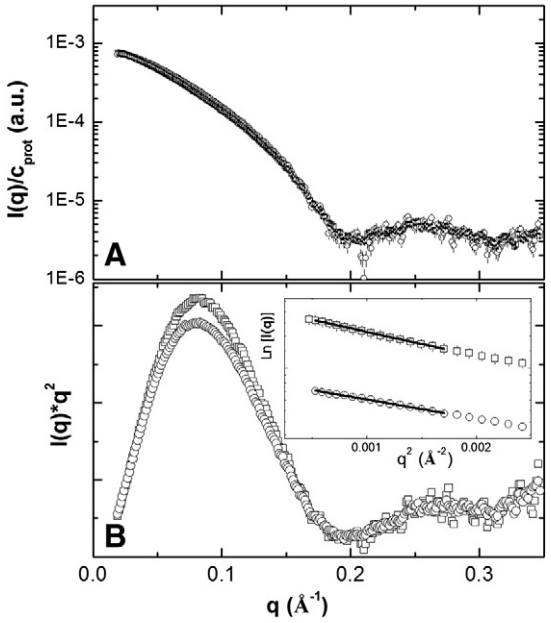


**Fig. 5.** Small angle X-ray scattering analysis of TLL. A. Concentration-normalized scattering intensity of TLL at 2.7 (circles) and 5.4 mg/mL (squares). B. Kratky plot of TLL scattering curves at 2.7 (open circles) and 5.4 mg/mL (open squares). Inset: Guinier plots at these two concentrations. More information about the Guinier analysis can be found in the Supplementary Material, Fig. S1.

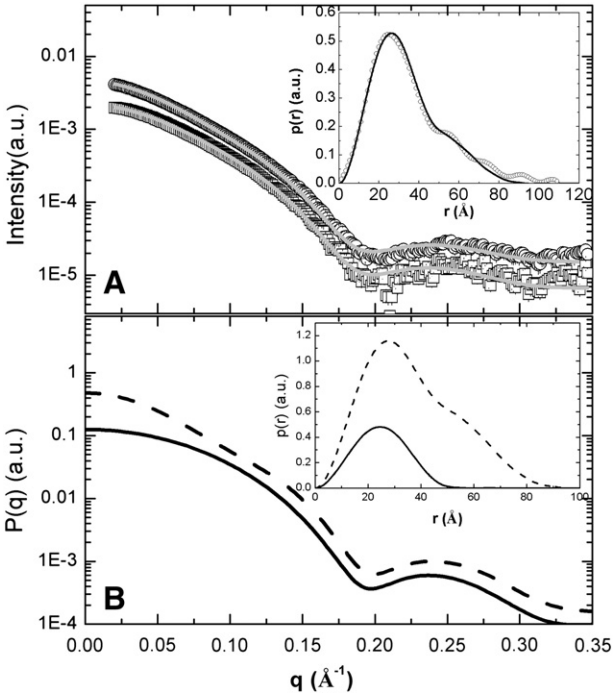


**Fig. 6.** Experimental and theoretical SAXS curves evidence the presence of dimers and monomers of TLL in solution. A. Scattering curve of TLL at 5.4 mg/mL (circles) and 2.7 mg/mL (squares) along with the best theoretical scattering intensity obtained with GENFIT software (solid lines) (see text for further details). The respective $p(r)$ function of TLL at 5.4 mg/mL obtained with the IFT methodology can be appreciated in the inset (open circles). B. Theoretical calculation using GENFIT [25] of TLL in the monomeric (solid line) and dimeric (dashed line) forms (PDB entry: 1DT3). The theoretical $p(r)$ functions of the monomer (solid line) and dimer (dashed line) can be appreciated in the inset of panel B. The solid line in the inset of panel A represents the weighted sum of the monomeric and dimeric theoretical $p(r)$ functions. See text for further details.

2.7 mg/mL, respectively (Fig. 5B, inset). We found no evidence of protein aggregation in the 2.7 to 5.4 mg/mL concentration range.

The IFT (Indirect Fourier Transform) methodology [50] is widely employed to study protein conformation in solution. The SAXS curve of TLL at 5.4 mg/mL (circles) along with the theoretical curve obtained with the IFT methodology (solid dark gray line) are shown in Fig. 6A. As the concentration-normalized scattering curves are quite similar (Fig. 5A), the IFT data analysis was made only with the scattering curve of TLL at 5.4 mg/mL. The correspondent normalized $p(r)$ (open circles in the inset of Fig. 6A) indicates that the protein presents a slightly anisometric shape with a cross-section of $35 \pm 3$ Å and a $D_{max} = 95 \pm 7$ Å. From the $p(r)$ function it is also possible to calculate the protein's $R_g$ value [11,17–19], which, in this case, was $28.23 \pm 0.15$ Å, in agreement with the value obtained using the Guinier approximation ($26.50 \pm 0.20$ Å).

The crystallographic structure of TLL (PDB: 1DT3) shows that, in the crystal, TLL self-assemble as dimers [2]. To check whether in solution TLL would have the same behavior as in the crystal, the theoretical protein form factors were evaluated using GENFIT software [25]. The protein crystallographic structure was used as the input (PDB: 1DT3) [2]. The calculated form factors of TLL for both monomer (solid line) and dimer (dashed line) are shown in Fig. 6B. Interestingly, for $q$ values larger than 0.075 $Å^{-1}$ the scattering curves have similar profiles, despite a scaling factor (Fig. 6B).

GENFIT software also calculates the respective $p(r)$ function of each monomeric (solid line) and dimeric (dashed line) TLL forms (Fig. 6B, inset). Interestingly, neither of these functions was able to reproduce the one obtained with the IFT methodology (open circles in the inset of Fig. 6A). This is an indication that the system is composed by a sum of monomers and dimers in solution.

Furthermore, the monomer and dimer $R_g$ values can be evaluated using the respective $p(r)$ functions [19]; according to this procedure, the obtained values are 19.0 and 28.2 Å for the monomer and dimer of TLL, respectively. The $R_g$ values obtained with the Guinier analysis are $26.50 \pm 0.20$ and $24.03 \pm 0.14$ Å for TLL at 5.4 and 2.7 mg/mL, respectively, suggesting that TLL is mostly dimeric at these conditions.

Next, we used the known monomer and dimer crystallographic structures to try to fit the SAXS data, assuming that the systems were composed by only one species, i.e., only monomers or dimers. Nevertheless, none of these configurations were able to reproduce the experimental scattering curves (Fig. S3). The next step was to use a combination of both monomers and dimers, assuming that they coexist in solution in equilibrium.

According to the SDS-PAGE and mass spectrometry analysis, both monomers and dimers could be present in solution. We evaluated the scattering curves as a sum of monomers and dimers using the appropriate weights [26] with the GENFIT software [22,23]. This software allows the use of different weights to each possible population (i.e., monomer or dimer), as described in the Materials and Methods section.

According to such procedure, the best fit (Fig. 6A, solid lines) obtained for TLL at 2.7 mg/mL (Fig. 6A, squares) and 5.4 mg/mL (Fig. 6A, circles) indicates that $43 \pm 2\%$ of the species are in the monomeric conformation, whereas $57 \pm 3\%$ of the protein is in the dimeric state for TLL at 2.7 mg/mL. At 5.4 mg/mL these values are $38.5 \pm 1.5\%$ and $61.5 \pm 1.4\%$ for monomer and dimer conformations, respectively. Besides, the reduced $\chi^2$ values [22,23,25,26] were equal to 1.7 and 2.3 for TLL at 2.7 and 5.4 mg/mL, respectively, indicating that a good fitting was obtained using the described methodology. Noteworthy, the amount of dimer slightly increases as the protein concentration increases what is consistent to a monomer/dimer equilibrium process.

Furthermore, these results show that the employed methodology was able to describe both scattering curves concomitantly, also elucidating the amount of protein in the monomeric and dimeric forms for each TLL concentration. Although the amount of protein in each state was rather similar for TLL at 2.7 and 5.4 mg/mL, the different methodologies utilized in this work revealed that the monomer/dimer ratio changes upon sample dilution/concentration.

Recently, Carvalho et al. [51] studied the temperature stability of extracellular hemoglobin of *Glossoscolex paulistus* at different oxidation

states by SAXS and dynamic light scattering measurements. To analyze the SAXS curves, the authors used a linear combination of the $p(r)$ functions to obtain information about the dissociation process. Following a similar procedure, the calculated values of $w_M$ and $w_D$ were 40 ± 2% and 60 ± 2%, respectively, in good agreement with the $w_M$ and $w_D$ values obtained with GENFIT. The respective $p(r)$ can be appreciated in the inset of Fig. 6A (solid black line).

### 3.5. Analysis of oligomeric and conformational distribution of TLL in solution by mass spectrometry

To further evaluate the oligomeric distribution of the TLL in solution we have used two mass spectrometry techniques. A solution analysis of TLL was performed by electrospray mass spectroscopy coupled with ion mobility spectroscopy technique (ESI–IMS–MS). The ESI–IMS–MS technique assists in the deconvolution of the spectral congestion typically observed in one-dimensional ESI–MS, allowing the separation of ions in a polydisperse complex sample showing varying oligomeric and conformational species with similar m/z [12–14]. In the present analysis performed in buffered aqueous solution at pH 7.0, we observed a predominant species corresponding to the monomeric TLL, with the corresponding ions with $z/n$ spanning from +28/1 to +10/1 (Fig. 7A). At higher drift time, a minor population was also observed, compatible with monomers with ions spanning from $z/n = +28/1$ to +15/1. At higher $m/z$ another ion envelope was detected, which is compatible with dimeric species of the TLL ($z/n = +20/2$ to +16/2) (Fig. 7A). The deconvolution of the molecular ions spectrum to a single charged monoisotopic mass spectrum evidences the monomer and dimer of TLL (Fig. 7B).

Further confirmation of the identity of the TLL was accessed by MALDI-ToF-MS (Fig. 7C). A major peak of about 29.4 kDa (for monocharged ion) was observed, compatible with the non-glycosylated form of TLL (expected molar mass from sequence: 29,315.5 Da; UNIPROT: O59952(23–291)). Other peaks in the MALDI-ToF mass spectra were observed for lower m/z, compatible with the +2 and +3 ions. A broad signal centered at about 31.5 kDa (for monocharged ion) was also observed, which is compatible with the monoglycosylated (at Asp33) form of the TLL, as previously reported elsewhere [3,52] (Fig. 7C). No further peaks from other components with dissimilar molecular mass were detected up to 70,000 m/z (not shown), indicating the high purity of the sample. These data demonstrate the complex behavior of the TLL enzyme in solution and the delicate balance between two monomeric conformers and a dimeric assembly.

In summary, our results strongly indicate that the lipase from *T. lanuginosus* is found as dimers and monomers co-existing in aqueous solution at the studied concentration range. Even at lower concentrations, the enzyme seems to maintain this oligomerization state (i.e. does not dissociates completely into monomers), as seen by the obtained $R_g$ values from the SAXS data and the ESI–IMS–MS analysis.

Bimolecular interaction was shown to be important to maintain enzyme stability, but it was reported that enzyme activity is reduced in the dimeric form [6,7]. Thus, even a small fraction of dimeric species would compromise overall enzyme activity, a factor that should be taken into account when applying this enzyme in industrial processes [8]. In general, high-concentrated solutions of the enzyme are used, meaning that the dimeric form will predominate over the monomeric form. As studied before for other lipases, the monomeric form is more active than the dimeric form; thus, the use of diluted lipase solutions or addition of detergents could increase the efficiency of the industrial processes. In contrast, in processes where high temperatures are needed, higher enzyme concentration is required, as the dimers are more thermal stable than the monomers, a fact evidenced for lipases from *Alcaligenes* sp. and *P. fluorescens* [6]. Therefore, it is of value to study the conformation and monomer/dimer ratio of such enzymes in different conditions.

## 4. Conclusions

Herein we evaluated the folding and conformation of *T. lanuginosus* lipase using different spectroscopic and mass spectrometry approaches. Circular dichroism and intrinsic fluorescence analysis showed that the investigated enzyme presented high thermal stability ($T_m$ of 73.6 ± 0.8 °C), and that the secondary structure changes were partially reversible, as described in previous studies. While chemical-induced unfolding with GdnHCl evidenced a two-state transition, with no suggestion of intermediate or different oligomeric states, an SDS-resistant dimeric specie was found by SDS-PAGE analysis. Mass spectrometry analysis after in-gel digestion of the bands from the SDS-PAGE identified the possible dimeric species as the TLL. Binding to 1,8 ANS indicated that TLL did not unfold completely even at high GdnHCl concentrations (6 M). To evaluate if TLL would be present as dimers and monomers in solution, SAXS curves of TLL at concentrations ranging from 27 to 2.7 mg/mL were obtained. The $p(r)$ calculated with the IFT methodology showed that TLL at 5.4 mg/mL presents an anisometric shape with a

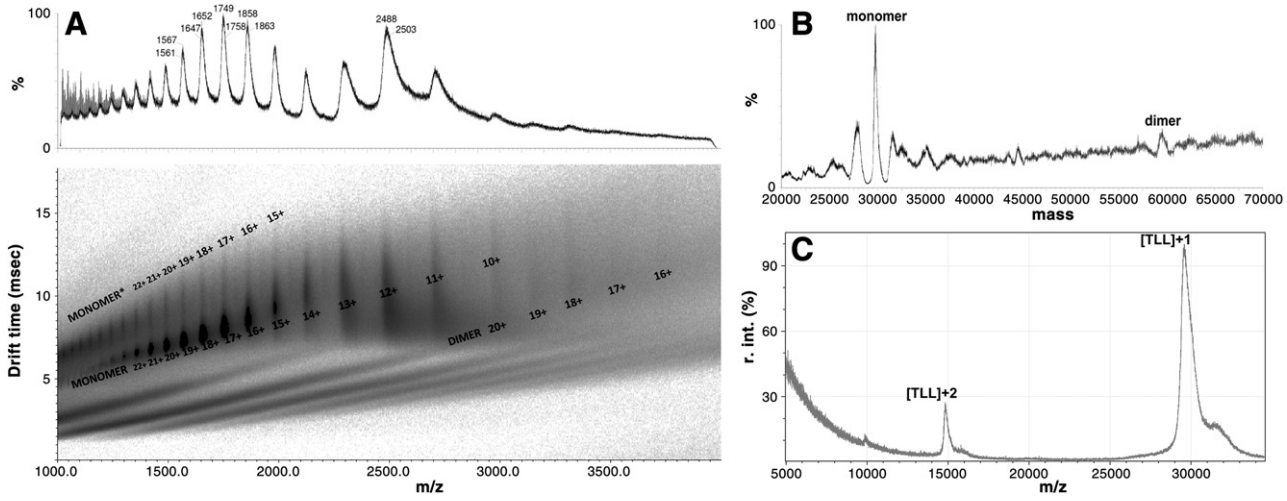


**Fig. 7.** Mass spectrometry analysis of TLL. A. TLL was subjected to ESI–MS coupled to IMS technique, in 100 mM aqueous ammonium acetate, pH 7.0, and the corresponding charge of each ion is identified with a number adjacent to them. In the top part, the summed ESI–MS spectrum is shown, evidencing the series of multiply charged ions. B. The deconvoluted ESI–MS spectrum evidences the monomer and the dimer of TLL in solution. C. MALDI-ToF-MS analysis of TLL. The TLL was subjected to MALDI-ToF-MS with sinapinic acid, allowing the identification of the +1, +2 and +3 ions. Details are described in the Material and Methods section.

$D_{max} = 95 \pm 7$ Å, and the obtained $R_g$ value was 28.23 ± 0.15 Å, similar to the one calculated from the Guinier regression (26.50 ± 0.20 Å). Theoretical calculations with GENFIT did not support the existence of only one TLL species in solution, i.e., both monomers and dimers should exist at the studied conditions. The best fit to the experimental SAXS curve was obtained supposing that the system was composed of monomers and dimers at different amounts and using GENFIT. According to such methodology, a mixture of monomers and dimers (around 40 ± 2% monomers and 60 ± 3% dimers) was obtained for TLL at both 2.7 and 5.4 mg/mL concentrations. Besides, ESI–IMS–MS analysis of SEC-eluted samples evidenced the presence of two monomeric conformations and a smaller fraction of a dimer of TLL. In summary, our results show that TLL is populated as both dimers and monomers in solution, mainly at higher concentrations, that might be relevant for its function.

In our work, the presence of both monomers and dimers of *T. lanuginosus* lipase (TLL) in solution was identified using a number of spectroscopic techniques. This study is relevant for the Biotechnology and Biocatalysis fields that include immobilization processes. Moreover, our work might also have future therapeutic impact, as stable forms of TL lipase are candidates for pancreatic enzyme replacement therapy [53]. In this case, the presence of dimers would reduce the therapeutic efficacy.

## Acknowledgments

This work was supported by grants from the Conselho Nacional de Desenvolvimento Científico e Tecnológico (CNPq); from the Instituto Nacional de Ciência e Tecnologia de Biologia Estrutural e Bioimagem (INBEB); Fundação de Amparo à Pesquisa do Estado do Rio de Janeiro (FAPERJ); Fundação de Amparo à Pesquisa do Estado de São Paulo (FAPESP); Coordenação de Aperfeiçoamento de Pessoal de Nível Superior (CAPES). This work has also been supported by the Brazilian Synchrotron Light Laboratory (LNLS) under proposals SAXS1-10913 and SAXS1-12664. LRSB thanks FAPESP and CNPq for financial support. The authors are in debt with Prof. Paolo Mariani and Francesco Spinozzi from *Università Politecnica delle Marche*, Italy who provided GENFIT software. We also thank Prof. Russolina B. Zingali, Augusto Vieira and Ana Carvalho (Unidade de Espectrometria de Massas de Proteínas, UEMP, UFRJ), and Eduardo R. dos Santos (CEMBIO-CCS-UFRJ) for excellent assistance with the mass spectrometry measurements and Dr. Priscila S. Ferreira for valuable assistance with the SEC analysis.

## Appendix A. Supplementary data

Supplementary data to this article can be found online at http://dx.doi.org/10.1016/j.bpc.2013.12.001.

## References

[1] R. Verger, Interfacial activation of lipases: facts and artifacts, Trends Biotechnol. 15 (1997) 32–38.
[2] M. Brzozowski, H. Savage, C.S. Verma, J.P. Turkenburg, D.M. Lawson, A. Svendsen, S. Patkar, Structural origins of the interfacial activation in *Thermomyces* (*Humicola*) *lanuginosa* lipase, Biochemistry 39 (2000) 15071–15082.
[3] C. Pinholt, M. Fano, C. Wiberg, S. Hostrup, J.T. Bukrinsky, S. Frokjaer, W. Norde, L. Jorgensen, Influence of glycosylation on the adsorption of *Thermomyces lanuginosus* lipase to hydrophobic and hydrophilic surfaces, Eur. J. Pharm. Sci. 40 (2010) 273–281.
[4] K. Zhu, A. Jutila, P.K.J. Kinnunen, Steady state and time resolved effects of guanidine hydrochloride on the structure of *Humicola lanuginosa* lipase revealed by fluorescence spectroscopy, Prot. Sci. 9 (2000) 598–609.
[5] K. Zhu, A. Jutila, E.K.J. Tuominen, P.K.J. Kinnunen, Effects of i-propanol on the structural dynamics of *Thermomyces lanuginosa* lipase revealed by tryptophan fluorescence, Prot. Sci. 10 (2001) 339–351.
[6] L. Wilson, J.M. Palomo, G. Fernández-Lorente, A. Illanes, J.M. Guisán, R. Fernández-Lafuente, Effect of lipase–lipase interactions in the activity, stability and specificity of a lipase from *Alcaligenes sp*, Enzyme Microb. Technol. 39 (2006) 259–264.
[7] G. Fernandez-Lorente, J.M. Palomo, M. Fuentes, C. Mateo, J.M. Guisan, R. Fernandez-Lafuente, Self-assembly of *Pseudomonas fluorescens* lipase into bimolecular aggregates dramatically affects functional properties, Biotechnol. Bioeng. 82 (2003) 232–237.
[8] J.M. Palomo, M. Fuentes, G. Fernandez-Lorente, C. Mateo, J.M. Guisan, R. Fernandez-Lafuente, General trend of lipase to self-assemble giving bimolecular aggregates greatly modifies the enzyme functionality, Biomacromolecules 4 (2003) 1–6.
[9] R. Fernandez-Lafuente, Lipase from *Thermomyces lanuginosus*: uses and prospects as an industrial biocatalyst, J. Mol. Catal. B Enzym 62 (2010) 197–212.
[10] J.E. Mogensen, P. Sehgal, D.E. Otzen, Activation, inhibition, and destabilization of *Thermomyces lanuginosus* lipase by detergents, Biochemistry 44 (2005) 1719–1730.
[11] D.I. Svergun, Small-angle scattering studies of macromolecular solutions, J. Appl. Crystallogr. 40 (2007) 10–17.
[12] B. Ruotolo, K. Giles, I. Campuzano, A.M. Sandercock, R.H. Bateman, C.V. Robinson, Evidence for macromolecular protein rings in the absence of bulk water, Science 310 (2005) 1658–1661.
[13] D.P. Smith, S.E. Radford, A.E. Ashcroft, Elongated oligomers in beta2-microglobulin amyloid assembly revealed by ion mobility spectrometry–mass spectrometry, Proc. Natl. Acad. Sci. U. S. A. 107 (2010) 6794–6798.
[14] L.C. Palmieri, M.P. Favero-Retto, D. Lourenco, L.M. Lima, A T(3)R(3) hexamer of the human insulin variant B28Asp, Biophys. Chem. 173–174C (2013) 1–7.
[15] M.M. Bradford, A rapid and sensitive method for the quantitation of microgram quantities of protein utilizing the principle of protein-dye binding, Anal. Biochem. 72 (1976) 248–254.
[16] G. Invernizzi, L. Casiraghi, R. Grandori, M. Lotti, Deactivation and unfolding are uncoupled in a bacterial lipase exposed to heat, low pH and organic solvents, J. Biotechnol. 141 (2009) 42–46.
[17] O. Glatter, O. Kratky, Small Angle X-ray Scattering, Academic Press, New York, 1982.
[18] L.A. Feigin, D.I. Svergun, Structure Analysis by Small-Angle X-Ray and Neutron Scattering, Plenum Press, Springer, 1987.
[19] G. Fournet, A. Guinier, Small Angle scattering of X-rays, John Wiley & Sons, New York, 1955.
[20] D.I. Svergun, A.V. Semenyuk, L.A. Feigin, Small-angle-scattering-data treatment by the regularization method, Acta Crystallogr. A 44 (1988) 244–250.
[21] D.I. Svergun, Determination of the regularization parameter in indirect-transform methods using perceptual criteria, J. Appl. Crystallogr. 25 (1992) 495–503.
[22] M.G. Ortore, F. Spinozzi, S. Vilasi, I. Sirangelo, G. Irace, A. Shukla, T. Narayanan, R. Sinibaldi, P. Mariani, Time-resolved small-angle x-ray scattering study of the early stage of amyloid formation of an apomyoglobin mutant, Phys. Rev. E. 84 (2011) 061904–061910.
[23] L.R.S. Barbosa, M.G. Ortore, F. Spinozzi, P. Mariani, S. Bernstorff, R. Itri, The importance of protein–protein interactions on the pH-induced conformational changes of bovine serum albumin: a small angle x-ray scattering study, Biophys. J. 98 (2010) 147–157.
[24] Website, accessed on August 13th 2013 http://www.isf.univpm.it/biophysics/software.htm.
[25] M.G. Ortore, F. Spinozzi, P. Mariani, A. Panciaroni, L.R.S. Barbosa, H. Amenitsch, M. Teinhart, J. Oliver, D. Russo, Combining structure and dynamics: non denaturating high-pressure effect on lysozyme in solution, J. R. Soc. Interface. 6 (2009) 619–634.
[26] L.R.S. Barbosa, F. Spinozzi, P. Mariani, R. Itri, Small-angle x-ray scattering applied to proteins in solution, Proteins in Solution and at Interfaces: Methods and Applications in Biotechnology and Materials Science, Wiley, New York, 2013.
[27] W.H. Press, S.A. Teukolsky, W.T. Vetterling, B.P. Flannery, Numerical Recipes: The Art of Scientific Computing, 3rd ed. Cambridge University Press, New York, 2007.
[28] M. Strohalm, M. Hassman, B. Kosata, M. Kodícek, mMass data miner: an open source alternative for mass spectrometric data analysis, Rapid Commun. Mass Spectrom. 22 (2008) 905–908.
[29] J.P. Williams, J.A. Lough, I. Campuzano, K. Richardson, P.J. Sadler, Use of ion mobility mass spectrometry and a collision cross-section algorithm to study an organometallic ruthenium anticancer complex and its adducts with a DNA oligonucleotide, Rapid Commun. Mass Spectrom. 23 (2009) 3563–3569.
[30] E.C.H.J. Michielsen, J.H.C. Diris, W.K.W.H. Wodzig, M.P.V. Dieijen-Visser, Size-exclusion chromatography of circulating cardiac troponin T, Clin. Chem. 52 (2006) 2306–2307.
[31] M. Wojdyr, Fityk: a general-purpose peak fitting program, J. Appl. Crystallogr. 43 (2010) 1126–1128.
[32] M.D. Abràmoff, P.J. Magalhães, S.J. Ram, Image processing with ImageJ, Biophoton. Int. 11 (7) (2004) 36–42.
[33] M. Fano, M.V. de Weert, E.H. Moeller, N.A. Kruse, S. Frokjaer, Ionic strength-dependent denaturation of *Thermomyces lanuginosus* lipase induced by SDS, Arch. Biochem. Biophys. 506 (2011) 92–98.
[34] F. Gentile, P. Amodeo, F. Febbraio, F. Picaro, A. Motta, S. Formisano, R. Nucci, SDS-resistant active and thermostable dimers are obtained from the dissociation of homotetrameric-glycosidase from hyperthermophilic Sulfolobus solfataricus in SDS, J. Biol. Chem. 277 (2002) 44050–44060.
[35] M. Galvis, O. Barbosa, R. Torres, C. Ortiz, R. Fernandez-Lafuente, Effect of solid-phase chemical modification on the features of the lipase from *Thermomyces lanuginosus*, Process Biochem. 47 (2012) 460–466.
[36] Ö. Aybastıer, C. Demir, Optimization of immobilization conditions of *Thermomyces lanuginosus* lipase on styrene–divinylbenzene copolymer using response surface methodology, J. Mol. Catal. B Enzym. 63 (2010) 170–178.
[37] L. Whitmore, B.A. Wallace, Protein secondary structure analyses from circular dichroism spectroscopy: methods and reference databases, Biopolymers 89 (2008) 392–400.
[38] N. Sreerema, R.W. Woody, A self-consistent method for the analysis of protein secondary structure from circular dichroism, Anal. Biochem. 209 (1993) 32–44.
[39] I.H.M. Van Stokkum, H.J.W. Spoelder, M. Bloemendal, R. Van Grondelle, F.C.A. Groen, Estimation of protein secondary structure and error analysis from CD spectra, Anal. Biochem. 191 (1990) 110–118.

[40] Y. Cordeiro, J. Kraineva, R. Ravindra, L.M. Lima, M.P. Gomes, D. Foguel, R. Winter, J.L. Silva, Hydration and packing effects on prion folding and beta-sheet conversion. High pressure spectroscopy and pressure perturbation calorimetry studies, J. Biol. Chem. 279 (2004) 32354–32359.
[41] K. Zhu, A. Jutila, E.K.J. Tuominen, S.A. Patkar, A. Svendsen, P.K.J. Kinnunen, Impact of the tryptophan residues of *Humicola lanuginosa* lipase on its thermal stability, Biochim. Biophys. Acta 1547 (2001) 329–338.
[42] H. Christensen, R.H. Pain, Molten globule intermediates and protein folding, Eur. Biophys. J. 19 (1991) 221–229.
[43] A.P. Bom, M.S. Freitas, F.S. Moreira, D. Ferraz, D. Sanches, A.M. Gomes, A.P. Valente, Y. Cordeiro, J.L. Silva, The p53 core domain is a molten globule at low pH: functional implications of a partially unfolded structure, J. Biol. Chem. 285 (2010) 2857–2866.
[44] A. Stobiecka, S. Wysocki, A.M. Brzozowski, Fluorescence study of fungal lipase from *Humicola lanuginosa*, J. Photochem. Photobiol. B 45 (1998) 95–102.
[45] A. Jutila, K. Zhu, E.K.J. Tuominen, P.K.J. Kinnunen, Fluorescence spectroscopic characterization of *Humicola lanuginosa* lipase dissolved in its substrate, Biochim. Biophys. Acta 1702 (2004) 181–189.
[46] J. Slavik, Anilino naphthalene sulfonate as a probe of membrane composition and function, Biochim. Biophys. Acta 694 (1982) 1–25.
[47] A. Hawe, M. Sutter, W. Jiskoot, Extrinsic fluorescent dyes as tools for protein characterization, Pharm. Res. 25 (2008) 1487–1499.
[48] A.M.D. Gonçalves, M.R. Aires-Barros, J.M.S. Cabral, Interaction of an anionic surfactant with a recombinant cutinase from *Fusarium solani pisi*: a spectroscopic study, Enzyme Microb. Technol. 32 (2003) 868–879.
[49] G.A. de Oliveira, E.G. Pereira, G.D. Ferretti, A.P. Valente, Y. Cordeiro, J.L. Silva, Intramolecular dynamics within the N-Cap-SH3-SH2 regulatory unit of the c-Abl tyrosine kinase reveal targeting to the cellular membrane, J. Biol. Chem. 288 (2013) 28331–28345.
[50] O. Glatter, A new method for the evaluation of small-angle scattering data, J. Appl. Crystallogr. 10 (1977) 415–421.
[51] J.W.P. Carvalho, P.S. Santiago, T. Batista, C.E.G. Salmon, L.R.S. Barbosa, R. Itri, M. Tabak, On the temperature stability of extracellular hemoglobin of *Glossoscolex paulistus* at different oxidation states: SAXS and DLS studies, Biophys. Chem. 163–164 (2012) 44–55.
[52] E. Boel, T. Christensen, H.F. Woldike, I.B. Huge-Jensen, *Humicola* lipase produced in *aspergillus*, US Patent 5 (1998) 766, 912.
[53] H. Wang, J. Hagedorn, A. Svendsen, K. Borch, D.E. Otzen, Variant of the *Thermomyces lanuginosus* lipase with improved kinetic stability: a candidate for enzyme replacement therapy, Biophys. Chem. 172 (2013) 43–52.